Journal of Coordination Chemistry

Insights into the N-terminal Cu(II) and Cu(I) binding sites of the human copper transporter CTR1

Yulia Shenberger, Ortal Marciano, Hugo E. Gottlieb & Sharon Ruthstein

Taylor & Francis
Taylor & Francis Group

Insights into the N-terminal Cu(II) and Cu(I) binding sites of the human copper transporter CTR1

Yulia Shenberger, Ortal Marciano, Hugo E. Gottlieb and Sharon Ruthstein

The Department of Chemistry, Faculty of Exact Sciences, Bar-Ilan University, Ramat-Gan, Israel

ABSTRACT

Copper transporter 1 (CTR1) is the main copper transporter in the eukaryotic system. CTR1 has several important roles: It binds Cu(II) ions that are present in the blood; it reduces those Cu(II) ions to Cu(I); and it subsequently transfers Cu(I) to the cytoplasmic domain, where the ion is delivered to various cellular pathways. Here, we seek to identify CTR1 binding sites for Cu(II) and Cu(I) and to shed light on the Cu(II)-to-Cu(I) reduction process. We focus on the first 14 amino acids of CTR1. This N-terminal segment is rich with histidine and methionine residues, which are known to bind Cu(II) and Cu(I), respectively; thus, this region has been suggested to have an important function in recruiting Cu(II) and reducing it to Cu(I). We utilize electron paramagnetic resonance (EPR) spectroscopy together with nuclear magnetic resonance (NMR) and UV-VIS spectroscopy and alanine substitution to reveal Cu(II) and Cu(I) binding sites in the focal 14-amino-acid segment. We show that H5 and H6 directly coordinate to Cu(II), whereas M7, M9, and M12 are involved in Cu(I) binding. This research is another step on the way to a complete understanding of the cellular copper regulation mechanism in humans.
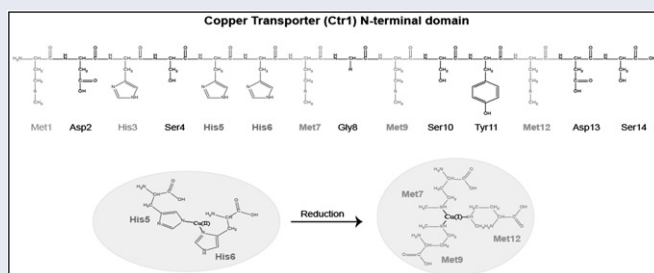
GRAPHICAL ABSTRACT

1. Introduction

Copper is an essential trace element for life and is used by all aerobic organisms as an enzyme-cofactor in various biochemical processes [1–11]. In a biological environment,

copper is found in two oxidation states: Cu(I) and Cu(II). Controlled redox cycling between these two states is what enables copper to be involved in the electron transfer reactions that underlie its important biological roles [7, 8]. Yet, this redox cycling can be deleterious to cells, because it catalyzes the production of reactive oxygen species (ROS) through Fenton/Haber–Weiss chemistry [10]. Beyond the potential toxicity associated with redox cycling, copper can exert additional toxic effects when it is present in the cell at excessive concentrations; since it is at the top of the Irving–Williams series [12], it may replace other essential metal ions in the cell such as iron.

To avoid these toxic effects, cells have developed a system to control the Cu(I)–Cu(II) cycling process and to regulate in-cell copper concentration. The copper transporter CTR1 is a key player in this system: Specifically, CTR1 binds Cu(II), reduces it to Cu(I), and subsequently transfers the Cu(I) to the cell [13, 14], where Cu(I) chaperones deliver the copper ion to specific cellular pathways [1, 9, 15–17]. Notably, the mechanism of the Cu(II)-to-Cu(I) reduction process is still not fully understood. In general, it has been suggested that copper metabolism is intimately linked to iron metabolism, and that copper and iron participate in each other's oxidation/reduction reactions. Indeed, in the yeast *Saccharomyces cerevisiae*, Cu(II) is reduced in the plasma membrane by Fre1 or Fre2 [18, 19], and can then be oxidized from Cu(I) to Cu(II) by Fet3 metalloxidase [20, 21]. In mammals, the process is more complex, and has not been resolved yet. One hypothesis is that it involves Dcytb and Steap proteins [22–24]. Herein, we seek to shed additional light on this reduction process by identifying CTR1 binding sites for Cu(II) and for Cu(I).

CTR1 is a trimer [25, 26], in which each monomer has a molecular weight of 23 kDa and comprises 190 amino acids. The reduction of Cu(II) to Cu(I) occurs at the extracellular, N-terminal domain of CTR1. This domain, comprising 60 residues, is rich with histidine and methionine residues [2, 27–29]. The Pearson chemical hardness (HSAB principle) predicts interaction of Cu(I) with cysteine, methionine, and histidine residues, and for Cu(II) binding with histidine residues [30]. Therefore, the N-terminal domain of CTR1 is adapted to bind both Cu(II) and Cu(I). The methionine residues are arranged in methionine-rich sequences called methionine segment (Mets) motifs. In general, such motifs, of the form MXXM and MXM, are present in a number of proteins involved in copper metabolism [31–38]. Mets motifs are capable of binding Cu(I) with micromolar affinity and may be responsible, in part, for recruiting Cu(I) to proteins in the cell [27]. Although they are highly selective, Mets motifs lack sequence specificity, aside from containing two/three methionine amino acids. The extracellular domain of CTR1 contains three Mets motif sites (M7-M9-M12; M40-M41-M42; M43-M45) and thus has the potential to coordinate at least three Cu(I) ions [27, 39]. The extracellular domain of CTR1 is also rich in histidine, which can bind both Cu(I) and Cu(II). Specifically, the domain contains two histidine-rich sites: The first involves H3, H5, and H6, and the second involves H22-H24 [14, 39].

Cell experiments suggest that the first 14 amino acids of the N-terminal domain of CTR1 (Figure 1) are essential for copper binding and reduction [35, 39]. This is owing to the spatial proximity between His-rich and Met-rich motifs, which are similar to the CopC protein of *Pseudomonas aeruginosa* [40]. In this prokaryotic protein, copper reduction accompanies its movement from the His-rich site to the Met-rich site.
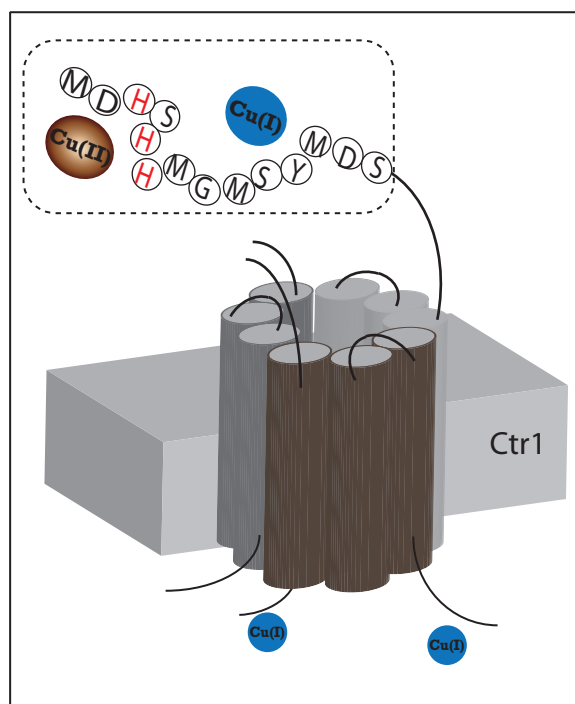
Figure 1. Schematic view presenting the first 14 amino acids of the copper transporter, CTR1.

Accordingly, several studies aiming to elucidate these processes have focused on this segment. In particular, Haas and colleagues used XAS experiments to study Cu(I) binding in this segment; they proposed that Cu(I) binds via N$_2$OS coordination to two His residues (the bis-His sequence, H5 and H6) and to a methionine residue [29]. Haas's group also used ultraviolet-visible spectroscopy (UV-VIS) experiments and preliminary electron paramagnetic resonance (EPR) measurements to study coordination of Cu(II) to the same 14-amino-acid segment [29, 41]. They revealed that H3 has an important role in preserving the segment's affinity for Cu(II) [29]. In addition, they showed that the bis-His sequence is significant for the Cu(II) reduction mechanism [29, 41]. Haas *et al.* [35] have also suggested in HEPES buffer, Cu(II) binding to the N-terminal domain of CTR1 involves 4N coordination, and that this coordination involves the ATCUN motif (NH$_2$ and H3) and the bis-His (H5 and H6) [41]. In a different study, Du *et al.* [33] used UV-VIS and calorimetric titration experiments to propose that the ATCUN motif and the bis-His sequence might be two different Cu(II) sites, and that Cu(I) prefers to bind to Met-rich motifs rather than to His-rich motifs.

Herein, in line with the studies cited above, we also focus on the first 14 amino acids of CTR1. We synthesized peptides matching this sequence, and introduced substitutions into several sites of interest (see Table 1 and Section 2 for further details). In order to resolve the coordination environment of Cu(II), we utilized titration continuous-wave (CW) and pulsed EPR experiments. EPR is the best method to characterize Cu(II) coordination to biomolecules, since it provides the direct Cu(II) coordination site without any modeling [42–47]. Titration EPR experiments allow differentiation between various states of the Cu(II): bound to a single biomolecule, bound to aggregate of

Table 1. Peptides studied in this research.

	Peptide sequence
Pep1_WT	MDHSHHMGMSYMDS
Pep2_G8A	MDHSHHMAMSYMDS
Pep3_H3A	MDASHHMGMSYMDS
Pep4_H5A	MDHSAHMGMSYMDS
Pep5_H6A	MDHSHAMGMSYMDS
Pep6_WT	MTSSL-CMDHSHHMGMSYMDSC-MTSSL
Pep7_M1A	MTSSL-CADHSHHMGMSYMDSC-MTSSL
Pep8_M7A	MTSSL-CMDHSHHAGMSYMDSC-MTSSL
Pep9_M9A	MTSSL-CMDHSHHMGASYMDSC-MTSSL
Pep10_M12A	MTSSL-CMDHSHHMGMSYADSC-MTSSL

biomolecules, or unbound Cu(II). In contrast to prior experiments targeting Cu(II)–CTR1 binding, which were carried out in HEPES buffer [29, 41], our experiments used KPi buffer. We found out that KPi constitutes a stable environment for the focal CTR1 segment, even at low temperatures, and can eliminate some confounding effects, as elaborated below. To explore Cu(I) coordination, we performed 1D and 2D nuclear magnetic resonance (NMR), together with pulsed EPR measurements and UV-VIS. We further used EPR to observe Cu(II) reduction to Cu(I) in the presence of ascorbate. Our experiments enable us to identify Cu(II) and Cu(I) binding sites at the molecular level, thereby providing potentially vital information regarding how the human copper transporter functions. Notably, our results shed new light on the mechanism of Cu(II) binding to the N-terminal domain of CTR1.

2. Materials and methods

2.1. Peptide synthesis, purification, and labeling

We focus on the first 14 amino acids of the extracellular, N-terminal domain of CTR1: MDHSHHMGMSYMDS. To identify Cu(II) and Cu(I) coordination sites, we synthesized a series of 10 peptides (Pep1–Pep10), as listed in Table 1. Pep1 (Pep1_WT) is made up of the wild-type sequence of the 14 residues. We synthesized Pep2–Pep5 to study coordination of Cu(II). As Cu(II) ions have preferences for His and Gly residues [48], each of the peptides Pep2–Pep5 is composed of the 14-residue sequence with a single substitution of either His or Gly with alanine. As Cu(II) is a paramagnetic metal ion, its coordination can be studied using CW-EPR spectroscopy [44, 49]. Cu(I), in contrast, is diamagnetic and EPR-silent. Thus, in order to be able to use EPR to study Cu(I) coordination, we synthesized peptides Pep6–Pep10 to include two cysteine residues, one at each terminus, to which we attached MTSSL ((1-Oxyl-2,2,5,5-tetramethyl-Δ3-pyrroline-3-methyl) methanethiosulfonate) spin labels. Pep6 (Pep6_WT) is composed of the spin-labeled wild-type 14-residue sequence. Cu(I) prefers to coordinate to Met residues; thus, in each of the peptides Pep7–Pep10, we substituted a single Met residue with alanine.

All peptides used in this study were synthesized on a rink amide resin (Applied Biosystems, Foster City, CA). Couplings of standard Fmoc (9-fluorenylmethoxy-carbonyl)-protected amino acids were achieved with *O*-(benzotriazol-1-yl)-*N,N,N′,N′*-tetramethyluronium hexafluorophosphate (HBTU, Dchem) in *N,N*-dimethylformamide (DMF, Bio-Lab) in combination with *N,N*-diisopropylethylamine (DIPEA, Bio-Lab) for a 1-h cycle. Fmoc deprotection was achieved with piperidine (Bio-Lab). Side-chain

deprotection and peptide cleavage from the resin were achieved by treating the resin-bound peptides with a 5-mL cocktail of 90% trifluoroacetic acid (TFA, Bio-Lab), 5% ethane dithiol (EDT, Alfa Aesar, Haverhill, MA), 2.5% triisopropylsilane (TIS, Alfa Aesar), and 2.5% thioanisole (Alfa Aesar), for 2.5 h under N_2. An additional 65 μL of bromotrimethylsilane (TMSBr, Alfa Aesar) were added during the final 30 min to minimize methionine oxidation. The peptides were washed four times with cold diethyl ether, vortexed, and then centrifuged for 5 min at 3500 rpm. After evaporation of TFA under N_2, 10 mM DTT (dithiothreitol, Sigma-Aldrich, St. Louis, MO) was added to the peptide, and it was dissolved in high-performance liquid chromatography (HPLC) water. The peptide was then purified using preparative reversed-phase HPLC (Vydac, C18, 5 cm). The mass of the peptide was confirmed either by MALDI-TOF MS-Autoflex III-TOF/TOF mass spectrometer (Bruker, Bremen, Germany) equipped with a 337-nm nitrogen laser, or with ESI (electron spray ionization) mass spectrometry on a quadruple time-of-flight (Q-TOF) low resolution micromass spectrometer (Waters Corp., Milford, MA). Peptide samples were typically mixed with two volumes of premade dihydrobenzoic acid (DHB) matrix solution, deposited onto stainless steel target surfaces, and allowed to dry at room temperature.

For site-directed spin labeling (SDSL): 1 mg lyophilized peptide was dissolved in 0.8 mL phosphate buffer (25 mM KPi) (pH = 7.3–7.4). 0.25 mg of S-(2,2,5,5-tetramethyl-2,5-dihydro-1H-pyrrol-3-yl)-methylmethanesulfonothioate) (MTSSL, TRC, Toronto, ON) dissolved in 15 μL dimethyl sulfoxide (DMSO, Bio-Lab) was added to the solution (50-fold molar excess of MTSSL). The spin-label and peptide solution were then vortexed overnight at 4 °C. The free spin-label was removed by semipreparative HPLC (Vydac, C18 1 cm). The mass of the spin-labeled peptide was confirmed by mass spectrometer (Figure S1).

2.2. Buffer preparation

KPi buffer: We preformed the EPR experiments at 25 mM, 50 mM, and 100 mM KPi buffer. We found that if the ratio between the peptide to the salt is larger than 25 the spectra are identical. The CW-EPR experiments presented here were performed with 1 mM peptide dissolved in 25 mM KPi. The ESEEM measurements were done with 1 mM peptide dissolved at 100 mM KPi. 25 mM KPi buffer was prepared as follows: 13.6 g KH_2PO_4 and 17.2 g K_2HPO_4 were dissolved in 4 L deuterium-depleted water, and titrated with NaOH until pH of 7.35 was achieved. For low temperature EPR measurements 10% glycerol was added to the solution to create a glass solution and was then freeze quenched to liquid N_2 temperature. Phosphate buffer were suggested to change their pH in the presence of sodium [50] while freezing, however, no indication to a change in pH in the presence of potassium was detected.

HEPES buffer: HEPES buffer (25 mM) was prepared as follows: 5.95 g HEPES was dissolved in 1 L deuterium-depleted water and titrated with NaOH until pH of 7.35 was achieved. For low temperature EPR measurements 10% glycerol was added to the solution.

2.3. Continuous-wave EPR

CW-EPR spectra were recorded using an E500 Elexsys Bruker spectrometer operating at 9.0–9.5 GHz equipped with a super-high-sensitivity CW resonator. The spectra were recorded at room temperature (RT, 295 ± 2 K) and at low temperature (130 ± 5 K) at microwave power of 20.0 mW, modulation amplitude of 1.0 G, a time constant of 80 ms, and receiver gain of 60.0 dB. The samples were measured in 1.0-mm capillary quartz tubes (VitroCom) at RT and in 4.0-mm quartz tubes (Wilmad-LabGlass, Vineland, NJ) at low temperature. CW-EPR simulations were carried out using MATLAB, with the EasySpin toolbox [51].

2.4. Cu(II) EPR reduction experiments

Cu(II) EPR reduction experiments were performed at RT as follows: 20 μL of $CuCl_2$ solution (2 mM in KPi buffer) was added to a peptide of interest (Pep1-5) (20 μL of 1 mM peptide in KPi buffer solution). At time zero, 20 μL of ascorbic acid (2 mM) was added, and the solution was mixed under anaerobic conditions. Cu(II) EPR signal intensity (at the maximum EPR signal intensity ($g_\perp$ position)) was measured as a function of time.

2.5. Cu(I) Addition to peptide solution

Cu(I) (Tetrakis(acetonitrile)copper(I) hexafluorophosphate) (Sigma-Aldrich) was added to a peptide solution under nitrogen gas to preserve anaerobic conditions. No Cu(II) EPR signal was observed at any time.

2.6. Electron spin echo envelope modulation (ESEEM) experiments

The 2P-ESEEM experiments and the 3P-ESEEM experiments were carried out at 10 ± 0.1 K on a Q-band Elexsys E580 spectrometer (equipped with a 2-mm probe head). The parameters for echo detected two-pulse experiment were $\tau = 200$ ns with $t(\pi/2) = 20$ ns, $dt = 10$ ns, and repetition time of 5 ms.

The three-pulse ESEEM experiments were performed as follows: A $\pi/2 - \tau - \pi/2 - T + dt - \pi/2 - \tau$ – echo sequence was used with a four-step phase-cycle. The $\pi/2$ pulse length was 20 ns, and the τ value was set to 220 ns to amplify ^{14}N modulations at $g_\perp$ position. The initial T was 100 ns and dt was 10 ns. The data were processed by subtracting the baseline using a polynomial fit. The resulting time domain was convoluted with hamming window function and the spectrum obtained by cross-term averaging Fourier transform [47, 52–54].

2.7. Constant-time four-pulse double electron electron resonance (DEER)

The DEER experiment $\pi/2(\nu_{obs}) - \tau_1 - \pi(\nu_{obs}) - t' - \pi(\nu_{pump}) - (\tau_1 + \tau_2 - t') - \pi(\nu_{obs}) - \tau_2 -$ echo was carried out at 80 ± 1.0 K on a Q-band Elexsys E580 spectrometer (equipped with a 2-mm probe head). A two-step phase cycle was employed on the first pulse. The echo was measured as a function of t', whereas τ_2 was kept constant to eliminate relaxation effects. The observer pulse was set at 60 MHz higher than the

pump pulse. The durations of the observer $\pi/2$ and π pulses were 40 ns each. The duration of the π pump pulse was 40 ns as well, and the dwell time was 20 ns. The observed frequency was 33.77 GHz. The power of the 40-ns π pulse was 20.0 mW; τ_1 was set to 200 ns and τ_2 to 1200 ns. Each set of DEER data was collected for 24 h. The spin concentration was between 0.1 and 0.2 mM. The samples were measured in 1.6-mm capillary quartz tubes (Wilmad-LabGlass). The data were analyzed using the DeerAnalysis 2015 program, with Tikhonov regularization [55]. We optimized the regularization parameter in the L curve by examining the fit of the time domain signal.

2.8. Nuclear magnetic resonance

NMR experiments were performed on a Bruker Avance-III-700 spectrometer equipped with a cryoprobe (700.5 and 176.1 MHz for ^{1}H and ^{13}C, respectively) in D_2O solutions at 300 K. The concentration of the peptide was 7 mM.

2.9. Ultraviolet-visible spectroscopy

UV-VIS measurements were performed using a Chirascan spectrometer (Applied Photophysics, Surrey, UK) at RT. Measurements were carried out in a 1-mm optical path length cell. The peptide concentration was 0.3 mg/mL. We observed difference absorption spectra of peptides titrated with Cu(I) from 200 to 600 nm with a step size and a bandwidth of 0.5 nm.

2.10. Computational simulation

We used Discovery Studio to build a model peptide with Cu(I) and Cu(II). We restrained the distances between Cu(I)/Cu(II) and the relevant amino acids that bind it using bond length parameters from the literature [37, 56–58]. We then optimized the structure to get an illustration of the system.

3. Results and discussion

3.1. Phosphate (KPi) buffer versus HEPES buffer

When exploring Cu(II) coordination to peptides, the choice of the buffer is important since it can affect the Cu(II) coordination. The literature reported various buffers when exploring Cu(II) coordination such as: HEPES, KPi, NEM, and Tris. Faller *et al.* have indicated that in Tris buffer the pH is dependent on the temperature, and therefore is not suitable for EPR measurements [50, 59]. KPi buffer and HEPES buffer were suggested to retain the coordination environment of Cu(II) at low temperature [50, 59]. Since Haas and coworkers have previously investigated the CTR1 N-terminal domain in HEPES buffer, we initially carried out low-temperature X-band (9 GHz) CW-EPR measurements in HEPES. However, we found out that Cu(II) is not well dissolved in HEPES, manifested by blue/purple color at the bottom of the vial. In addition, when increasing Cu(II) concentration, the spectrum becomes broad and not resolved, suggesting that also the peptide is aggregating in the presence of Cu(II) [Figure 2(a)]. In contrast,
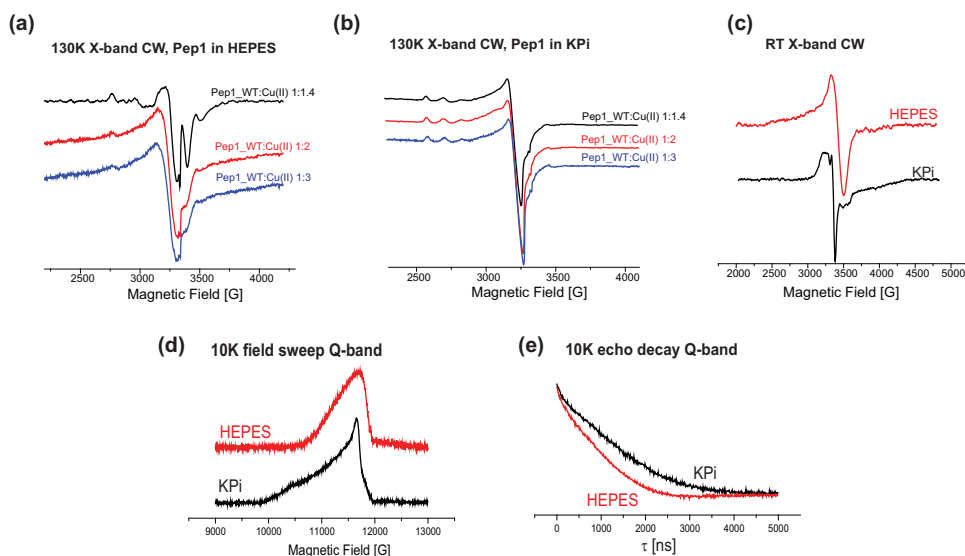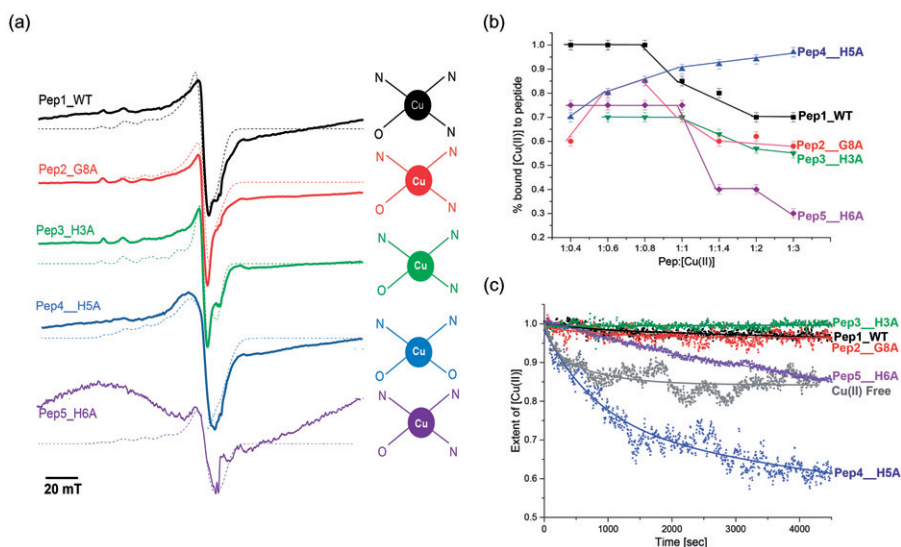
Figure 2. (a) Low temperature (130 ± 5 K) X-band CW-EPR spectra of Pep1 dissolved in HEPES buffer at various Cu(II) concentration. (b) Low temperature (130 ± 5 K) X-band CW-EPR spectra of Pep1 dissolved in KPi buffer at various Cu(II) concentration. (c) RT X-band CW-EPR spectra of Pep1 dissolved in HEPES and KPI buffer, where Cu(II):Pep1 ratio was 2:1. (d) 2P-field sweep Q-band carried out at 10 K, 33.84 ± 0.05 GHz of Pep1 dissolved in HEPES and KPi buffers where Cu(II):Pep1 ratio was 2:1. (e) 2P-ESEEM-band carried out at 10 K, 33.84 ± 0.05 GHz of Pep1 dissolved in HEPES and KPi buffers where Cu(II):Pep1 ratio was 2:1. Peptide concentration is 1 mM.

in phosphate, KPi buffer, Cu(II) coordination is stable at various Cu(II) concentrations, and the spectrum is well resolved, suggesting no peptide aggregation occurs at this concentration range [Figure 2(b)]. We also measured the Pep1 in HEPES and KPi buffers at RT [Figure 2(c)], which indicated that in KPi, the spectrum is much more resolved than in HEPES even at RT, proposing that Cu(II)-Pep1 aggregates can even form at RT in HEPES buffer. In order to confirm this, we also carried out pulsed EPR experiments at Q-band (33.8 GHz). The field sweep spectra of Pep1 in KPi and HEPES buffer at 10 K are presented in Figure 2(d), again showing less resolved spectrum in HEPES than in KPi. In addition the relaxation time of Cu(II) in HEPES is much faster than in KPi [Figure 2(e)], suggesting that aggregates are indeed formed in HEPES buffer. Considering all these, we chose to preform our EPR measurements in KPi buffer and not in HEPES buffer.

3.2. Cu(II) coordination to CTR1 N-terminal segment

To investigate Cu(II) binding to the extracellular domain of CTR1, for each of the peptides Pep1–Pep5 (Table 1), we carried out a series of CW-EPR measurements at 130 K in the presence of different concentrations of Cu(II). The data were subsequently incorporated into simulations using the EasySpin tool box, and the first coordination sphere of Cu(II) was determined for each peptide [44]. Figures S2–S6 in the SI show all experimental and simulated data, and the parameters derived from the simulations. Figure 3(a) shows the experimentally-obtained and simulated EPR spectra for Pep1–Pep5 for

Figure 3. (a) Low temperature (130 ± 5 K) CW-EPR spectra of 1:1 Cu(II) bound to Pep1–Pep5 (solid line), and their simulated spectra (dashed line). The parameters of each simulated spectrum are listed in the SI. (b) % of bound Cu(II) as a function of Pep:Cu(II) ratio. (c) Cu(II) reduction in the presence of ascorbate for: Cu(II) dissolved in buffer and Cu(II) dissolved in Pep1–Pep5 KPi buffer solutions. Peptide concentration is 1 mM.

[Cu(II)]:[Peptide] at a ratio of 1:1. The simulation for each peptide took into account two Cu(II) species. The first species corresponds to free Cu(II) ions in water, where Cu(II) is coordinated to four oxygens (4O coordination), with $g_{||} = 2.39 \pm 0.005$, $A_{||} = 154 \pm 2.0\,G$. The second species corresponds to Cu(II) that is bound to the peptide with coordination of 3N1O or 2N2O. Figure 3(a) shows that the spectra differ across the various peptides, suggesting that each substitution had an effect on Cu(II) coordination. Specifically, the EPR spectra of Cu(II) coordinated to either Pep4 or Pep5 are much broader than the other EPR spectra, indicating that the substitutions H5A and H6A each led to peptide aggregation in the presence of Cu(II). The simulation results suggest that Cu(II) binds to Pep1 (the WT sequence) with 3N1O coordination. This coordination is preserved in the presence of G8A (Pep2), H3A (Pep3), and H6A (Pep5) substitutions. However, for the H5A substitution (Pep4), Cu(II) binds with 2N2O coordination. This observation suggests that H5 is an essential residue for Cu(II) coordination.

Figure 3(b) shows, for each of the peptides Pep1–Pep5, the percentage of bound Cu(II) as a function of the [Peptide]:[Cu(II)] ratio. For Pep1, at low Cu(II) concentrations, all Cu(II) is bound, suggesting high affinity of Cu(II) to Pep1. Haas *et al.* observed similarly high affinity between Cu(II) and wild-type CTR1 [35]. Addition of Cu(II) to the Pep1 solution increased the percentage of free Cu(II), as expected. The G8A mutation (Pep2) decreased the peptide's affinity to Cu(II), and the maximum percentage of bound Cu(II) in the presence of Pep2 was 80%, obtained at a ratio of Pep2:Cu(II) of 1:0.8. The H5A mutation (Pep4) achieved 100% bound Cu(II) only at a high Cu(II) concentration (Pep:Cu(II) of 1:3), also suggesting a lower affinity of Cu(II) to this peptide

variant, compared with the wild-type peptide. In addition, the low resolution of the CW-EPR spectrum suggests that more than one Cu(II) ion is bound to the peptide that eventually leads to aggregation of the peptide. In the presence of the H3A substitution (Pep3) and the H6A substitution (Pep5), only about 70% of the Cu(II) was able to bind at a ratio of 1:1 [Peptide]:[Cu(II)].

Next, we investigated the effects of the Pep2–Pep5 substitutions on the reduction of Cu(II) to Cu(I) (which is EPR-silent). To this end, we followed at RT the change in EPR intensity with time [Figure 3(c)]. The reduction was carried out in the presence of 2 mM ascorbate ([Peptide]:[Ascorbate]:[Cu(II)] ratio 1:2:2). For comparison, we also measured the reduction of free Cu(II) in buffer. Cu(II) in the presence of Pep1, Pep2, and Pep3 was quite stable, and only about 5% of the Cu(II) was reduced within 4000 s. This observation suggests tight binding of Cu(II), which hinders the capacity of the ascorbate to reach Cu(II), achieving a controlled reduction. Interestingly, for Pep4 (H5A), the reduction was rapid, faster than that of free Cu(II) ions. As noted above, Pep4 was characterized by a broader and less resolved CW-EPR spectrum [Figure 3(a)] compared with the other peptide variants, suggesting that it may form aggregates in the presence of Cu(II). In this situation the Cu(II) site may be unstable and incomplete and therefore is more exposed to external nucleophilic attack, which facilitates Cu(II) reduction. The H6A substitution was also characterized by more rapid Cu(II) reduction, as compared with Pep1. These results provide further support to the notion that H5 and H6 are directly involved in coordination of Cu(II).

3P-ESEEM experiments were performed in order to evaluate the interaction between the electron spin with nearby (∼2–6 Å) nuclei. These nuclei are typically not directly coordinated to the metal ion but lie on the residue that is directly bound to the metal ion. Therefore, ESEEM experiments are good for targeting the remote nitrogen in an imidazole ring that is directly coordinated to Cu(II) [47, 52–54]. Figure 4 presents the ESEEM time domain signals and the corresponding FT spectra for Pep1_WT, Pep3_H3A, Pep4_H5A, and Pep5_H6A. The ESEEM signals and FT spectra for Pep1_WT and Pep3_H3A are identical, confirming that H3 is not directly coordinated to Cu(II). In contrast, the ESEEM signals of Pep4_H5A and Pep5_H6A are different than Pep1_WT, showing less intense ^{14}N modulations. EasySpin simulations using the saffron function were conducted to evaluate the number of remote ^{14}N nuclei [dashed lines in Figure 4(b)]. Pep1_WT was simulated using two ^{14}N nuclei with the following quadrupole parameters: $e^2qQ/h = 1.44$ MHz, $\eta = 0.5$ for one nucleus and $e^2qQ/h = 1.44$ MHz, $\eta = 0.35$ for the other nuclei. Pep4_H5A was simulated with one ^{14}N nucleus ($e^2qQ/h = 1.44$ MHz, $\eta = 0.5$), and Pep5_H5A was simulated as well with one ^{14}N nucleus ($e^2qQ/h = 1.44$ MHz, $\eta = 0.35$).

Taken together, the results of these experiments suggest that residues H5 and H6 are directly coordinated to Cu(II) and are important for preserving high affinity of Cu(II), and that alterations at G8 and H3 affect Cu(II) affinity to CTR1. The significance of the H3 residue for preserving CTR1 affinity to Cu(II) is in line with the findings of Haas *et al.*, as discussed above [35]. Although G8 does not participate in direct binding to Cu(II), it might be important for preserving the correct flexibility of the peptide chain, and therefore point mutation at this residue affects Cu(II) affinity.
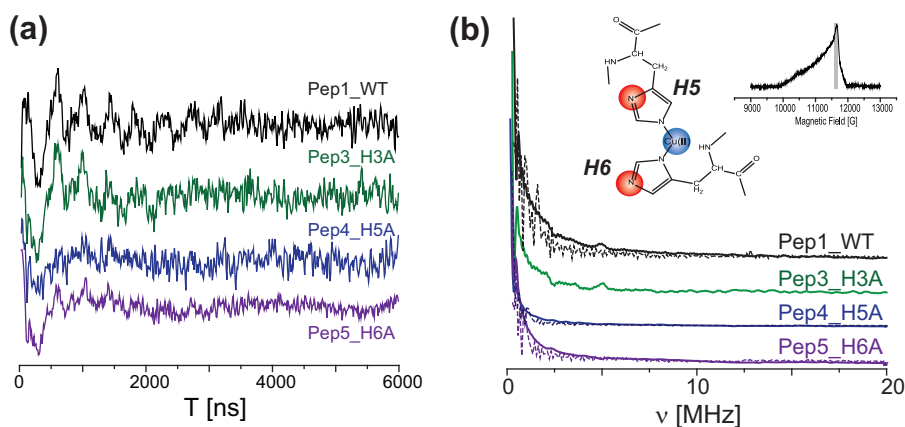
Figure 4. (a) Time domain ESEEM signals for Pep1_WT, Pep3_H3A, Pep4_H5A, and Pep5_H6A. (b) Corresponding ESEEM spectra. The dashed lines are simulated spectra. The inset spectrum shows the magnetic field position where the ESEEM where conducted, and an illustration of Cu(II) binding of H5 and H6 is presented as well.

3.3. Cu(I) coordination to CTR1 N-terminal segment

We carried out a ^{1}H NMR experiment on the Pep1_WT form in D$_2$O, in addition to several 2D experiments (COSY, NOESY) in a 700 MHz NMR spectrometer. In order to observe the amide NH signals, ^{1}H spectra (1D, TOCSY, and NOESY) were also run in 90% H$_2$O with water suppression. The amino-acid sequence was confirmed by observation in the HMBC spectrum (long-range ^{1}H × ^{13}C correlation) of interactions between the carbonyl carbons not only with intra-residue α and β protons, but also with the α protons of the adjacent residue in the chain. This process enabled us to assign signals to most of the amino acids in the peptide. The results are presented in Table 2. Addition of Cu(I) to the WT peptide caused shifts in the ^{1}H spectrum (Figure S7). The

Table 2. ^{1}H NMR chemical shifts after the addition of Cu(I) to Pep1.

| Position		NH H	+Cu(I)	α H	+Cu(I)	β H	+Cu(I)	γ H	+Cu(I)	δ H	+Cu(I)
1	M	8.55	d	4.10	4.05(**)	2.06, 2.13		2.46		2.063[b]	
2	D	8.76	8.70(**)	4.64	>4.6	2.72					
3	H	8.80	8.70(*)	4.75	>4.6	3.14, 3.37	3.12, 3.35	7.33 (δ)	7.27	8.64 (ζ)	8.51[c](*)
4	S	8.42	8.38	4.33	4.29	3.80	3.79				
5	H	8.49	8.49	4.67	>4.6	3.11, 3.25	3.12, 3.24	7.27 (δ)	7.24	8.59 (ζ)	8.53[c](**)
6	H	8.56	d	4.65	>4.6	3.13, 3.22	3.12, 3.24	7.26 (δ)	7.24	8.59 (ζ)	8.53[c](**)
7	M	8.54	d	4.47	4.54(**)	1.98, 2.07		2.49, 2.56		2.061[b]	
8	G	8.51	8.48	3.94, 4.01	3.92, 3.99						
9	M	8.25	7.88(*)	4.49	4.53	1.95, 2.03	1.95, d	2.49, 2.53		2.067	
10	S	8.37	8.44(**)	4.41	4.44	3.79	3.79				
11	Y	8.16	8.14	4.53	4.50	2.95, 3.02	2.81(*), 3.01	7.08 (δ)	7.08	6.79 (ε)	8.82
12	M	8.11	7.88(**)	4.37	4.38	1.90, 2.02		2.38, 2.44		2.055	
13	D	8.29	8.22(**)	4.68	>4.6	2.78, 2.89	d, 2.81				
14[a]	S	8.20	8.11(*)	4.38	4.38	3.83, 3.90	3.82, 3.89				

[a]^{14}NH$_2$: 7.15 → 7.11, 7.59 → 7.53(**).
[b,c]Signals with the same superscript may be interchanged.
[d]Location of signal not determined.
* numbers: $\Delta\delta \geq 0.09$ ppm; ** numbers: $0.08 > \Delta\delta \geq 0.05$ ppm.
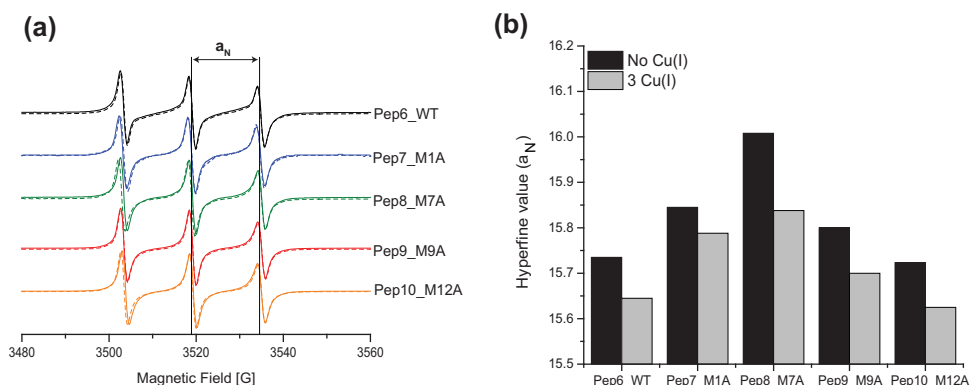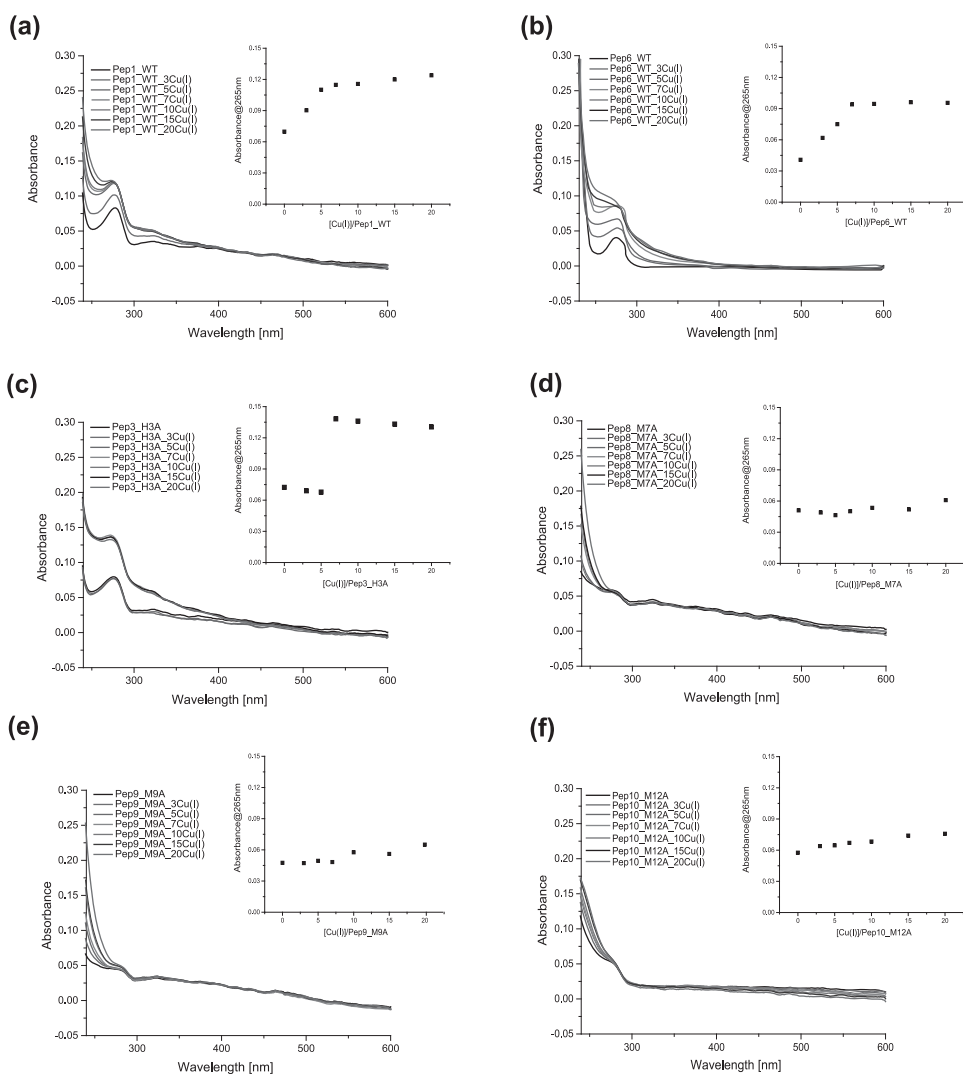
Figure 5. (a) RT CW-EPR spectra of spin-labeled Pep6–Pep10 in the presence (dashed line) and absence of Cu(I) (solid line). (b) The change in the hyperfine value (a_N) as a function of Pep:Cu(I) ratio. The error in a_N is ±0.05 G.

most significant changes occurred near His and Met residues (shown in color in Table 2), suggesting that these are the most relevant residues for Cu(I) binding in this peptide, as previously suggested by Haas's group [29, 41]. The largest shifts were observed for H3, M7, M9, and M12.
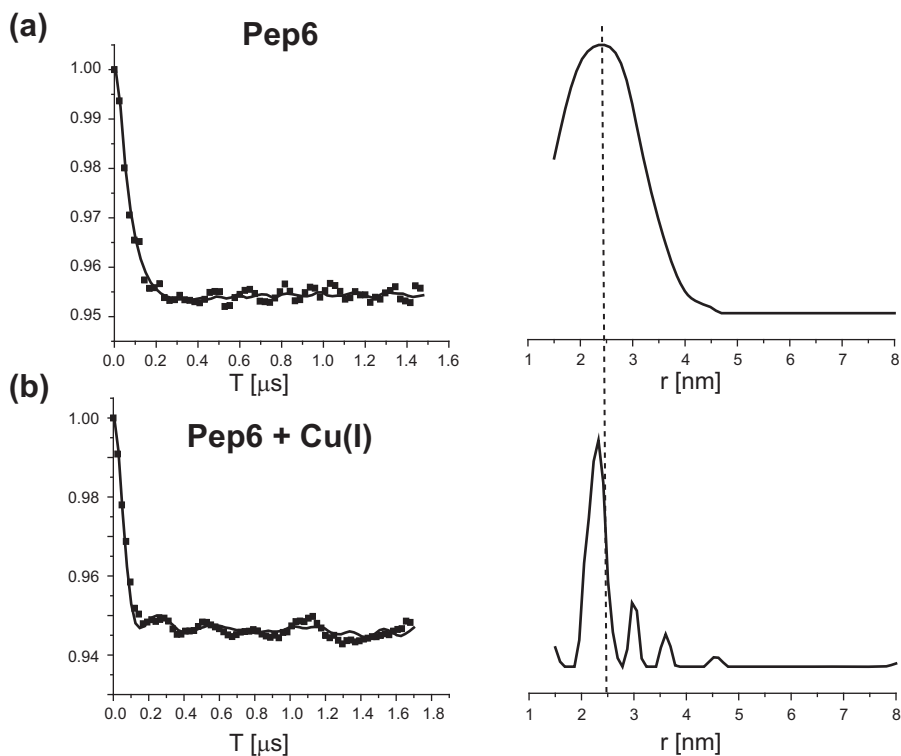

Figure 6. Q-band DEER signals for spin-labeled Pep6_WT, and corresponding distance distribution functions obtained from Tikhonov regularization in the absence of Cu(I) (a) and in the presence of Cu(I) (b).

Figure 7. UV-VIS absorbance spectra of (a) Pep1, (b) Pep6, (c) Pep3, (d) Pep8, (e) Pep9, and (f) Pep10 titrated with Cu(I). Insets: The change in absorbance at 265 nm for the various peptides as a function of [Cu(I)].

RT CW-EPR spectra of the spin-labeled peptides (Pep6–Pep10) were recorded [Figure 5(a)] in the presence and absence of Cu(I). The presence of Cu(I) was not associated with any substantial changes in the signals. However, closer analysis reveals that upon Cu(I) introduction, each peptide showed a slight broadening of the signal and a decrease in the hyperfine value (a_N). The broadening of the signal suggests that the two termini of each peptide get closer to each other upon Cu(I) binding. The decrease in the hyperfine value following Cu(I) introduction, a phenomenon that we have observed previously for other segments containing Met [60], suggests that, upon Cu(I) coordination, the spin-labels shift to point to a somewhat more hydrophobic environment. Figure 5(b) plots the hyperfine value as a function of the presence of Cu(I) ([Peptide]:[Cu(II)] ratio of 1:3) versus the absence of Cu(I). In the absence of Cu(I),
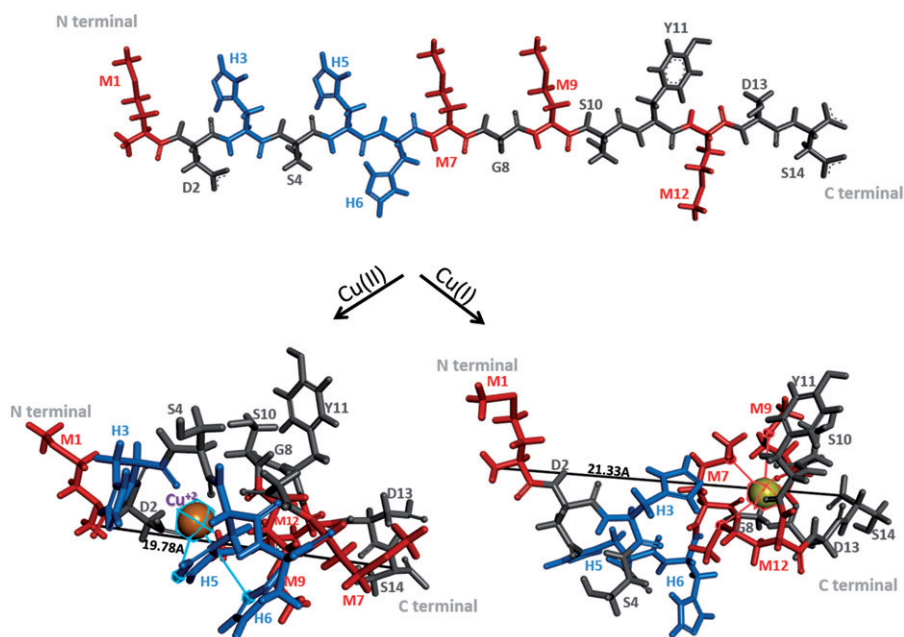
Figure 8. Illustration of Cu(I) and Cu(II) coordination to Pep1_WT. His residues are colored in blue; Met residues are colored in red. The black lines mark the N- to C-terminal distance.

the a_N value varies slightly across the different peptide variants, suggesting that each substitution has a slight effect on the folding of the peptide. In the presence of Cu(I), the largest change in the hyperfine value (as compared with its value in the absence of Cu(I)) is observed for Pep8 (M7A), suggesting that M7 is involved in Cu(I) coordination.

To trace the structural changes of Pep6_WT upon addition of Cu(I), we took DEER measurements in the absence and presence of Cu(I) (at a ratio of Pep6:[Cu(I)] of 1:3) (Figure 6). DEER is a pulsed EPR technique that can measure the dipolar interaction between two paramagnetic centers, thereby providing a distance distribution function in the range of 2.0–8.0 nm [61, 62]. The DEER measurements on Pep6 suggest that the distance between the two termini of the peptide is 2.5 ± 0.7 nm. Addition of Cu(I) to the solution results in a much narrower distance distribution function, as is also manifested by the clear time domain modulations in the DEER signal. The distance distribution obtained for Pep6 in the presence of Cu(I) is 2.3 ± 0.2 nm. The decrease in the average distance is in agreement with the slight broadening of the RT CW-EPR spectra observed in the previous experiment. These observations suggest that, upon Cu(I) coordination, the peptide becomes much more rigid and confined in space.

Taken together, the NMR and EPR data suggest that H3, M7, M9, and M12 play a role in Cu(I) coordination, and that upon Cu(I) coordination, the CTR1 N-terminal peptide becomes less flexible.

In order to gain further insight into Cu(I) coordination, we performed UV-VIS measurements on the various peptides. Figure 7 presents UV-VIS absorbance spectra for Pep1, Pep3, Pep6, and Pep8–Pep10, titrated with Cu(I). Titration of Cu(I) into the peptides led to the appearance of a peak at 265 nm, which is probably due to S → Cu

charge transfer transitions [27, 33]. At 265 nm, Pep1_WT showed an increase in absorption as Cu(I) concentration increased, indicating Cu(I) binding to the peptide; absorption reached a plateau at a ratio of 1:3 [Pep1]:[Cu(I)]. Pep6 (spin-labeled WT) showed a similar response to an increase in Cu(I) concentration, indicating that the addition of spin-labels to the peptide did not affect its copper binding properties. Pep3 showed a different pattern of absorption compared with Pep1_WT (and Pep6): binding occurred only at a [Cu(I)]:[Pep3_H3A] ratio exceeding 5.0. This observation indicates that Cu(I) affinity to Pep3_H3A is lower than its affinity to Pep1. Pep8–Pep10 did not show any change in absorbance upon Cu(I) addition. These results demonstrate the importance of M7, M9, and M12 to the binding of Cu(I).

4. Conclusion

EPR measurements, including titration and reduction experiments of Cu(II), enabled us to identify the Cu(II) coordination sphere in several variants of a peptide comprising the first 14 residues of CTR1. Although the focal peptide is only a short segment of the full copper transporter trimer, it has been shown to have a crucial role in Cu(II) recruiting and reduction mechanisms in the CTR1 N-terminal domain [29, 35, 41].

We observed that the H3, H5, H6, and G8 residues participate in Cu(II) binding, and that, specifically, H5 and H6 are included in Cu(II)'s direct coordination site. Notably, our results suggest that Cu(II) coordination to the focal 14-amino-acid segment of CTR1 corresponds to a 3N1O environment. This observation contrasts with the conclusions of Haas and colleagues, who suggested that Cu(II) binds to the 14-amino-acid segment via 4N coordination [35]. The authors proposed that the ATCUN motif (the N-terminal amine and H3) and the bis-His site (H5 and H6) are both directly coordinated to Cu(II), whereas our results indicate that the bis-His site is more important for Cu(II) coordination than H3 is. These differences may stem from the fact that Haas *et al*. have not explored the role of each histidine residue to Cu(II) coordination via point mutations, CW and pulsed EPR experiments. Moreover, the group has not considered that peptide aggregation can occur and it is dependent on the Cu(II) concentration. Therefore titration experiments at various Cu(II) concentrations are required to verify the correct Cu(II) coordination environment. We found that at specific Cu(II) concentration, the probability of Cu(II)-peptide aggregation is higher in HEPES buffer than in KPi buffer. Therefore, it is likely that the 4N coordination observed in previous studies was driven by Cu(II) binding to multiple peptides. Since CTR1 is a trimer, it might be that in the full membrane protein, Cu(II) can be found in 4N coordination, but this coordination involves H5 and H6 residues, and not the ATCUN motif as was suggested before. These observations highlight the importance of using multiple experimental methods and carefully monitoring the effects of buffer and Cu(II) concentration in order to resolve Cu(II) coordination.

For Cu(I) coordination, NMR measurements showed that, in the presence of Cu(I), the most substantial chemical shifts in the wild-type peptide occurred near His and Met residues, suggesting that H3, M7, M9, and M12 are the most relevant residues for Cu(I) binding in this peptide. RT CW-EPR spectra of spin-labeled peptides (Pep6–Pep10) in the presence of Cu(I) suggest that M7 is involved in Cu(I)

coordination. DEER measurements on Pep6 further indicate that, upon Cu(I) coordination, the peptide becomes much more rigid and confined in space. Finally, UV-VIS experiments confirmed the importance of M7, M9, and M12 to the binding of Cu(I).

Again, our observations diverge somewhat from those of Haas and colleagues. Their studies, which relied on XAS experiments, suggested that, in HEPES buffer, Cu(I) binds to the CTR1 N-terminal segment in an N_2OS coordination, and that H5 and H6 and one of the methionine residues are involved in this coordination [29]. Our measurements were not able to detect this coordination. The discrepancy between our results and the XAS data might be attributable to the difference in the buffer conditions or may indicate that there are two Cu(I) coordination sites in the first 14 amino acids of CTR1 with different affinities. Given that our results showed that Cu(II) is directly coordinated to H5 and H6, one possibility is that the Cu(I) site that involves H5, H6 and one of the methionine residues (which was resolved by XAS data) is an intermediate site that is formed during the reduction process from Cu(II) to Cu(I).

In eukaryotic and prokaryotic systems, Cu(I) has been found to be cycled between cysteine sites (involving two cysteine residues, i.e. CXXC), or between Mets segments [31, 63–66]. In proteins that can coordinate both Cu(II) and Cu(I) such as CopC and CopK [40, 67], Cu(II) sites involve His residues while Cu(I) sites involve Met residues. Likewise, computational study has suggested that Cu(I) is cycled between one Mets site and another in CTR1 [65]. Taking all this together, we propose that the Cu(I) site targeted in this study that involves the three methionine residues M7, M9, and M12 is the first stable binding site in the CTR1 N-terminal domain.

Figure 8 presents an illustration of Cu(II) and Cu(I) binding to Pep1_WT. This figure suggests that Cu(II) binding is closer to the N-terminal region of Pep1, whereas Cu(I) is concentrated in the C-terminal region of Pep1 as expected.

Disclosure statement

The authors report no potential conflict of interests.

Funding

References

1. S. Puig, D.J. Thiele. *Curr. Opin. Chem. Biol.*, **6**, 171 (2002).
2. A.E. Palmer, K.J. Franz. *Chem. Rev.*, **109**, 4533 (2009).
3. E. Madsen, J.D. Gitlin. *Annu. Rev. Neurosci.*, **30**, 317 (2007).
4. S. Lutsenko. *Curr. Opin. Chem. Biol.*, **14**, 211 (2010).
5. A.K. Boal, A.C. Rosenzweig. *Chem. Rev.*, **109**, 4760 (2009).
6. J.Y. Uriu-Adams, C.L. Keen. *Mol. Aspects Med.*, **26**, 268 (2005).
7. W. Cerpa, L. Varela-Nallar, A.E. Reyes, A.N. Minniti, N.C. Inestrosa. *Mol. Aspects Med.*, **26**, 405 (2005).
8. E. Gaggelli, H. Kozlowski, D. Valensin, G. Valensin. *Chem. Rev.*, **106**, 1995 (2006).
9. J.L. Burkhead, K.A.G. Reynolds, S.E. Abdel-Ghany, C.M. Cohu, M. Pilon. *New Phytol.*, **182**, 799 (2009).

10. J.H. Kaplan, S. Lutsenko. *J. Biol. Chem.*, **284**, 25461 (2009).
11. C.J. Feo, S.G. Aller, V.M. Unger. *BioMetals*, **20**, 705 (2007).
12. H. Irving, R.J.P. Williams. *J. Chem. Soc.*, 3192 (1953).
13. J. Lee, M.M.O. Pena, Y. Nose, D.J. Thiele. *J. Biol. Chem.*, **277**, 4380 (2002).
14. J.F. Eisses, J.H. Kaplan. *J. Biol. Chem.*, **277**, 29162 (2002).
15. N.J. Robinson, D.R. Winge. *Annu. Rev. Biochem.*, **79**, 537 (2010).
16. A.C. Rosenzweig. *Acc. Chem. Res.*, **34**, 119 (2001).
17. Z. Xiao, A.G. Wedd. *Chem. Commun.*, 588 (2002). doi: 10.1039/B111180A
18. R. Hassett, D.J. Kosman. *J. Biol. Chem.*, **270**, 128 (1995).
19. E. Georgatsou, L.A. Mavrogiannis, G.S. Fragiadakis, D. Alexandraki. *J. Biol. Chem.*, **272**, 13786 (1997).
20. C. Askwith, D. Eide, A. Van Ho, P.S. Bernard, L. Li, S. Davis-Kaplan, D.M. Sipe, J. Kaplan. *Cell*, **76**, 403 (1994).
21. A. Dancis, D.S. Yuan, D. Haile, C. Askwith, D. Eide, C. Moehle, J. Kaplan, R.D. Klausner. *Cell*, **76**, 393 (1994).
22. M.D. Knutson. *Nutr. Rev.*, **65**, 335 (2007).
23. L. Quintanar, C. Stoj, A.B. Taylor, P.J. Hart, D.J. Kosman, E.I. Solomon. *Acc. Chem. Res.*, **40**, 445 (2007).
24. A.T. Mckie, D. Barrow, G.O. Latunde-Dada, A. Rolfs, G. Sager, E. Mudaly, M. Mudaly, C. Richardson, D. Barlow, A. Bomford. *Science*, **291**, 1755 (2001).
25. C.J. De Feo, S.G. Aller, G.S. Siluvai, N.J. Blackburn, V.M. Unger. *Proc. Natl. Acad. Sci. U.S.A*, **106**, 4237 (2009).
26. S.G. Aller, V.M. Unger. *Proc. Natl. Acad. Sci. U.S.A.*, **103**, 3627 (2006).
27. Z. Xiao, F. Loughlin, G.N. George, G.J. Howlett, A.G. Wedd. *J. Am. Chem. Soc.*, **126**, 3081 (2004).
28. A. Godt, C. Franzen, S. Veit, V. Enkelmann, M. Pannier, G. Jeschke. *J. Org. Chem.*, **65**, 7575 (2000).
29. M.J. Pushie, K. Shaw, K.J. Franz, J. Shearer, K.L. Haas. *Inorg. Chem.*, **54**, 8544 (2015).
30. R.G. Parr, R.G. Pearson. *J. Am. Chem. Soc.*, **105**, 7512 (1983).
31. A.K. Wernimont, D.L. Huffman, L.A. Finney, B. Demeler, T.V. O'halloran, A.C. Rosenzweig. *J. Biol. Inorg. Chem.*, **8**, 185 (2003).
32. E. Wang, Z. Xi, Y. Li, L. Li, L. Zhao, G. Ma, Y. Liu. *Inorg. Chem.*, **52**, 6153 (2013).
33. X. Du, H. Li, X. Wang, Q. Liu, J. Ni, H. Sun. *Chem. Commun., (Camb.)* **49**, 9134 (2013).
34. J.P. Fabisiak, V.A. Tyurin, Y.Y. Tyurina, G.G. Borisenko, A. Korotaeva, B.R. Pitt, J.S. Lazo, V.E. Kagan. *Arch. Biochem. Biophys.*, **363**, 171 (1999).
35. K.L. Haas, A.B. Putterman, D.R. White, D.J. Thiele, K.J. Franz. *J. Am. Chem. Soc.*, **133**, 4427 (2011).
36. J. Jiang, I.A. Nadas, M.A. Kim, K.J. Franz. *Inorg. Chem.*, **44**, 9787 (2005).
37. J.T. Rubino, P. Riggs-Gelasco, K.J. Franz. *J. Biol. Inorg. Chem.*, **15**, 1033 (2010).
38. Y. Shenberger, V. Yarmiayev, S. Ruthstein. *Mol. Phys.*, **111**, 2980 (2013).
39. J.F. Eisses, J.H. Kaplan. *J. Biol. Chem.*, **280**, 37159 (2005).
40. M. Koay, L. Zhang, B. Yang, M.J. Maher, Z. Xiao, A.G. Wedd. *Inorg. Chem.*, **44**, 5203 (2005).
41. S. Schwab, J. Shearer, S.E. Conklin, B. Alies, K.L. Haas. *J. Inorg. Biochem.*, **158**, 70 (2016).
42. B.-K. Shin, S. Saxena. *J. Phys. Chem. B.*, **115**, 15067 (2011).
43. Z. Yang, M.R. Kurpiewski, M. Ji, J.E. Townsend, P. Mehta, L. Jen-Jacobson, S. Saxena. *Proc. Natl. Acad. Sci. U.S.A.*, **109**, E993 (2012).
44. J. Peisach, W.E. Blumberg. *Arch. Biochem. Biophys.*, **165**, 691 (1974).
45. E. Aronoff-Spencer, C.S. Burns, N.I. Avdievich, G.J. Gerfen, J. Peisach, W.E. Antholine, H.L. Ball, F.E. Cohen, S.B. Prusiner, G.L. Millhauser. *Biochemistry*, **39**, 13760 (2000).
46. M. Chattopadhyay, E.D. Walter, D.J. Newell, P.J. Jackson, E. Aronoff-Spencer, J. Peisach, G.J. Gerfen, B. Bennett, W.E. Antholine, G.L. Millhauser. *J. Am. Chem. Soc.*, **127**, 12647 (2005).
47. S. Ruthstein, K.M. Stone, T.F. Cunningham, M. Ji, M. Cascio, S. Saxena. *Biophys. J.*, **99**, 2497 (2010).

48. C. Migliorini, A. Sinicropi, H. Kozlowski, M. Luczkowski, D. Valensin. *J. Biol. Inorg. Chem.*, **19**, 635 (2014).
49. J. Peisach, W.E. Blumberg, E.T. Lode, M.J. Coon. *J. Biol. Chem.*, **246**, 5877 (1971).
50. P. Faller, C. Hureau, P. Dorlet, P. Hellwig, Y. Coppel, F. Collin, B. Alies. *Coord. Chem. Rev.*, **256**, 2381 (2012).
51. S. Stoll, A. Schweiger. *J. Magn. Reson* **178**, 42 (2006).
52. F. Jiang, J. Mccracken, J. Peisach. *J. Am. Chem. Soc.*, **112**, 9035 (1990).
53. C.S. Burns, E. Aronoff-Spencer, C.M. Dunham, P. Lario, N.I. Avdievich, W.E. Antholine, M.M. Olmstead, A. Vrielink, G.J. Gerfen, J. Peisach. *Biochemistry*, **41**, 3991 (2002).
54. G.J. Yeagle, M.L. Gilchrist, L.M. Walker, R.J. Debus, R.D. Britt. *Philos. Trans. R. Soc. Lond. B, Biol. Sci.*, **363**, 1157 (2008).
55. G. Jeschke. *Chemphyschem*, **3**, 927 (2002).
56. T.D. Tullius, P. Frank, K.O. Hodgson. *Proc. Natl. Acad. Sci. U.S.A.*, **75**, 4069 (1978).
57. B.T. Op't Hol, K.M. Merz. *Biochemistry*, **46**, 8816 (2007).
58. A.L. Pitts, M.B. Hall. *Inorg. Chem.*, **52**, 10387 (2013).
59. S.C. Drew, C.L. Masters, K.J. Barnham. *PLoS One*, **5**, e15875 (2010).
60. Y. Shenberger, H.E. Gottlieb, S. Ruthstein. *J. Biol. Inorg. Chem.*, **20**, 719 (2015).
61. A. Milov, A. Maryasov, Y.D. Tsvetkov. *Appl. Magn. Res.*, **15**, 107 (1998).
62. M. Pannier, S. Veit, A. Godt, G. Jeschke, H.W. Spiess. *J. Magn. Res.*, **142**, 331 (2000).
63. A.K. Boal, A.C. Rosenzweig. *J. Am. Chem. Soc.*, **131**, 14196 (2009).
64. I. Anastassopoulou, L. Banci, I. Bertini, F. Cantini, E. Katsari, A. Rosato. *Biochemistry*, **43**, 13046 (2004).
65. M. Schushan, Y. Barkan, T. Haliloglu, N. Ben-Tal. *Proc. Natl. Acad. Sci. U.S.A*, **107**, 10908 (2010).
66. A.N. Skvortsov, E.A. Zatulovskii, L.V. Puchkova. *Mol. Biol.*, **46**, 335 (2012).
67. M.-R. Ash, L.X. Chong, M.J. Maher, M.G. Hinds, Z. Xiao, A.G. Wedd. *Biochemistry*, **50**, 9237 (2011).